

**Al-doped  $\alpha$ -MnO<sub>2</sub> coated by lignin for high-performance rechargeable aqueous  
zinc-ion battery**

Jingliang Xu<sup>a,b,c</sup>, Xinhang Hu<sup>a</sup>, Md. Asraful Alam<sup>a</sup>, Gul Muhammad<sup>a</sup>, Yongkun Lv<sup>a</sup>,  
Minghai Wang<sup>a</sup>, Chenjie Zhu<sup>d</sup>, Wenlong Xiong<sup>a,\*</sup>

<sup>a</sup> *School of Chemical Engineering, Zhengzhou University, Zhengzhou 450001, China*

<sup>b</sup> *Zhengzhou Tuoyang Industrial Co., Ltd, Zhengzhou, China*

<sup>c</sup> *Zhengzhou University Industrial Technology Research Institute Co., Ltd, Zhengzhou,  
China*

<sup>d</sup> *College of Biotechnology and Pharmaceutical Engineering, Nanjing Tech  
University, 30 S Puzhu Rd, 211816 Nanjing, China*

**\*Corresponding Author**

Wenlong Xiong

E-mail: xiongwenlong@zzu.edu.cn

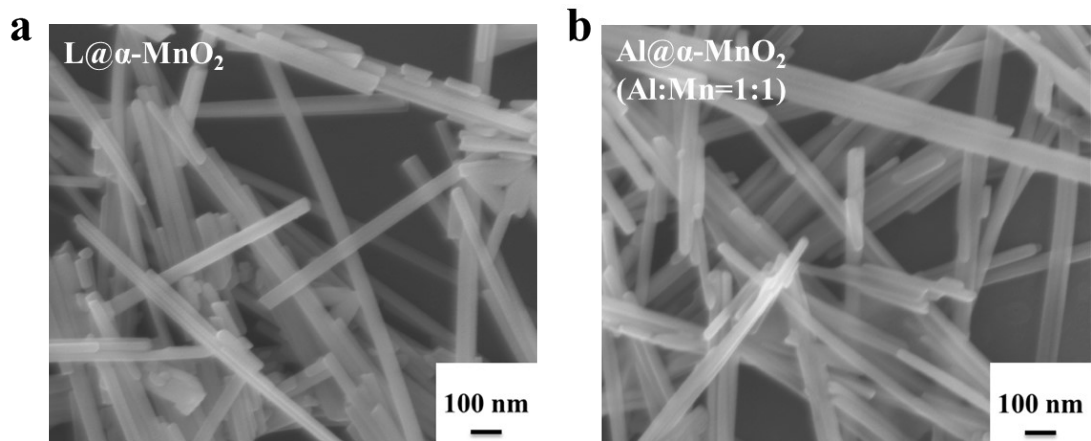


Figure S1 SEM of (a)  $α\text{-MnO}_2$  coated by lignin and (b)  $\text{MnO}_2$  doped by Al, Al:Mn=1:1.

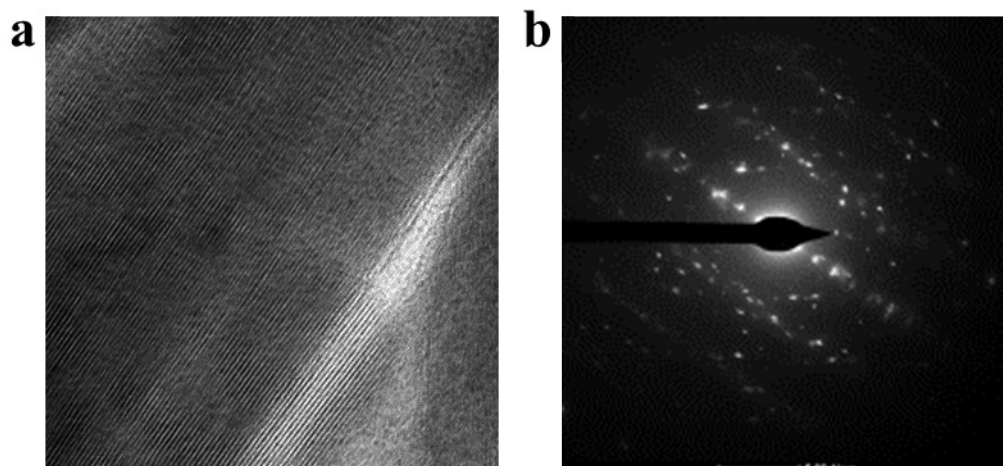


Figure S2 (a) HRTEM image and (b) SAED of L+Al@ $\alpha$ -MnO<sub>2</sub>

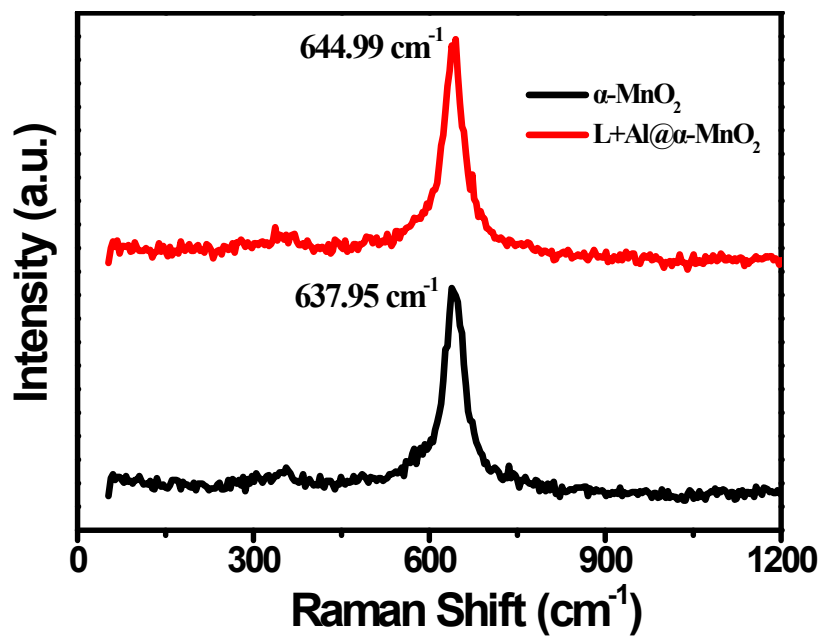


Figure S3 Raman spectra of  $\alpha\text{-MnO}_2$  and  $\text{L+Al@}\alpha\text{-MnO}_2$ .

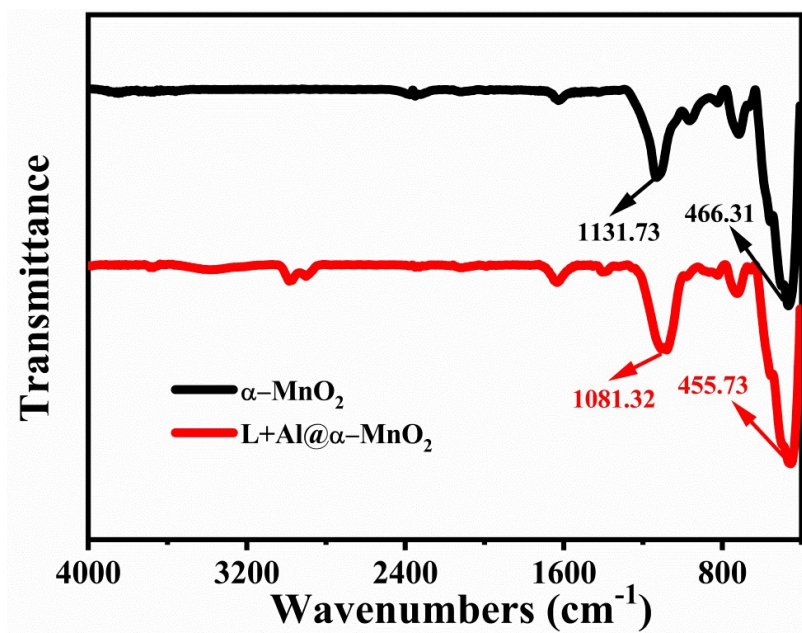


Figure S4 FT-IR spectrum of  $\alpha$ -MnO<sub>2</sub> and L+Al@ $\alpha$ -MnO<sub>2</sub>.

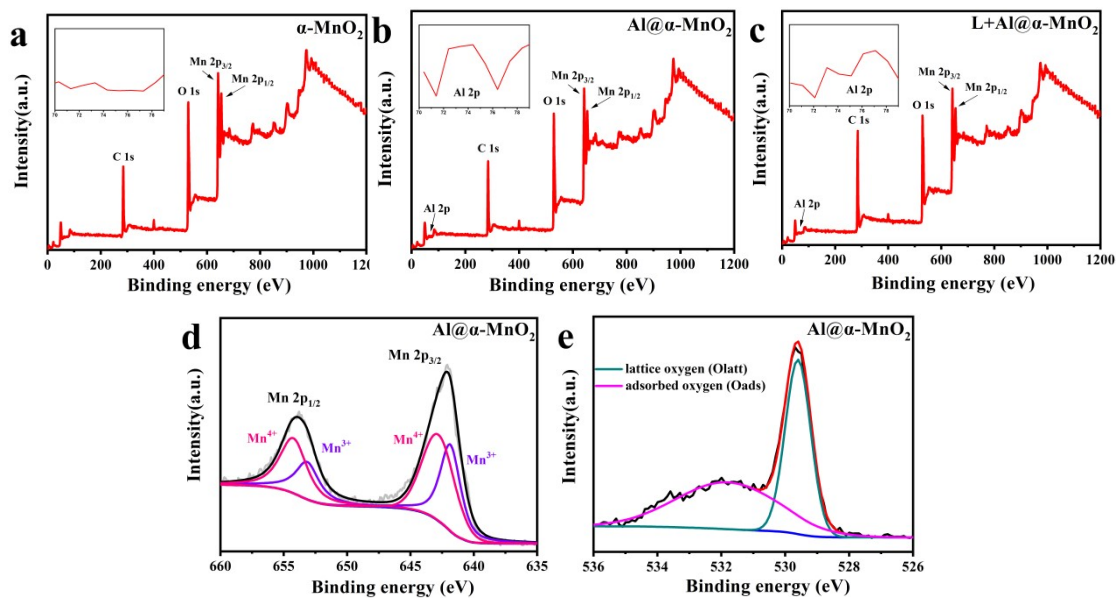


Figure S5 (a) XPS spectrum of  $\alpha$ -MnO<sub>2</sub>. (b) Al@ $\alpha$ -MnO<sub>2</sub> and (c) L+Al@ $\alpha$ -MnO<sub>2</sub>. (d)

Mn 2p spectrum of Al@ $\alpha$ -MnO<sub>2</sub> and (e) O 1s spectrum of Al@ $\alpha$ -MnO<sub>2</sub>.

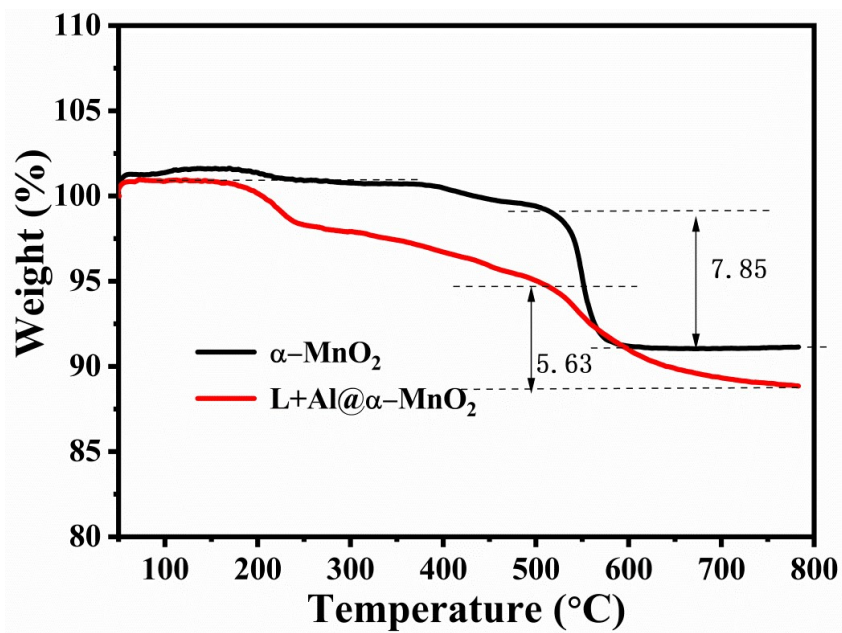


Figure S6 TG analysis of  $\alpha\text{-MnO}_2$  and  $\text{L+Al@}\alpha\text{-MnO}_2$ .

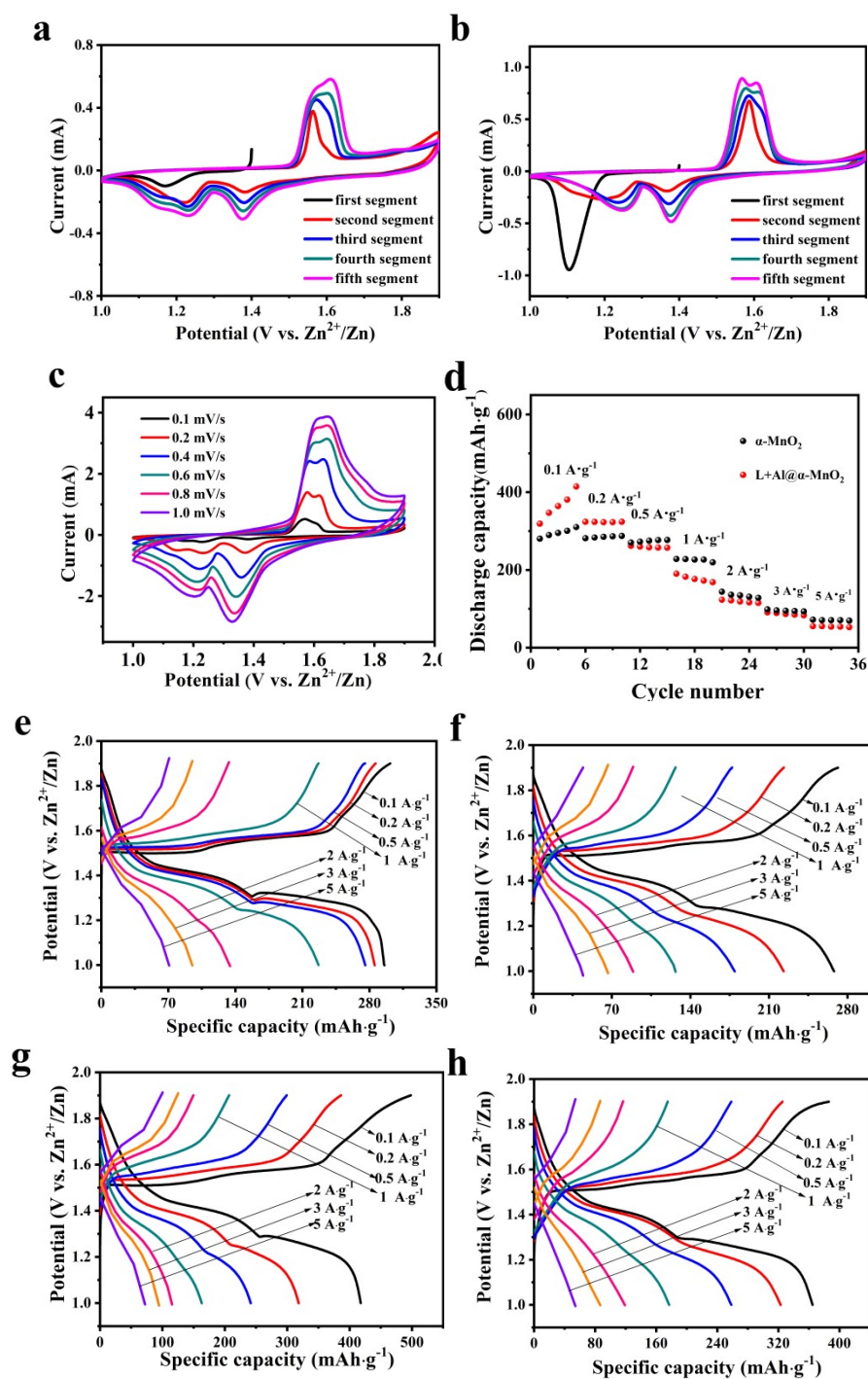


Figure S7 (a), (b) Cyclic voltammetry curves of Al@ $\alpha$ -MnO<sub>2</sub> and L@ $\alpha$ -MnO<sub>2</sub> at 0.1 mV·s<sup>-1</sup>. (c) CV curves of  $\alpha$ -MnO<sub>2</sub> at different sweep rates. (d) Rate performance of batteries using  $\alpha$ -MnO<sub>2</sub> and L+Al@ $\alpha$ -MnO<sub>2</sub> as the cathode material, respectively. (e), (f), (g) and (h) Charge-discharge profiles of batteries using  $\alpha$ -MnO<sub>2</sub>, Al@ $\alpha$ -MnO<sub>2</sub>, L@ $\alpha$ -MnO<sub>2</sub> and L+Al@ $\alpha$ -MnO<sub>2</sub> at the current densities varying from 0.1 to 5 A·g<sup>-1</sup>, respectively.



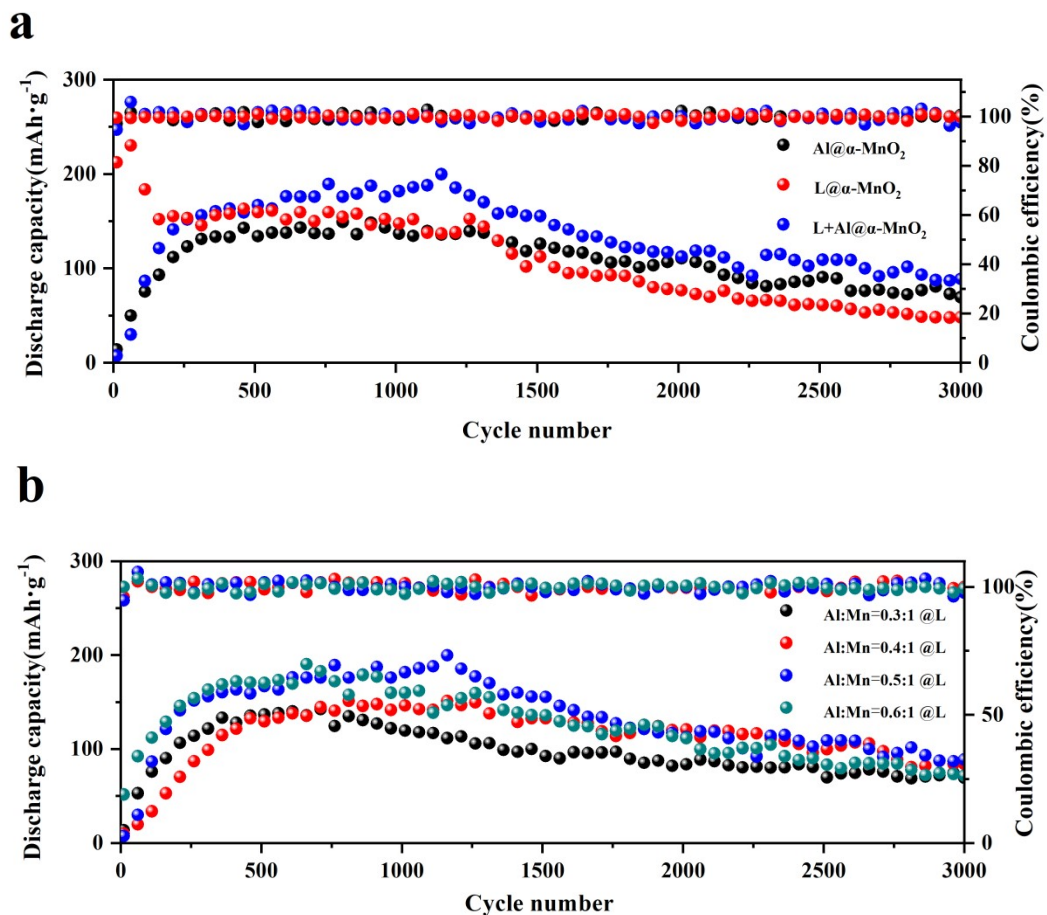


Figure S8 (a) Cycle performance of  $\text{Al@}\alpha\text{-MnO}_2$ ,  $\text{L@}\alpha\text{-MnO}_2$  and  $\text{L+Al@}\alpha\text{-MnO}_2$  at  $1.5\text{A}\cdot\text{g}^{-1}$ . (b) Cycle performance of  $\text{L+Al@}\alpha\text{-MnO}_2$  with different different initial molar ratios of Al and Mn at  $1.5\text{A}\cdot\text{g}^{-1}$ .